

The timing of sea ice formation and exposure to photosynthetically active radiation along the Western Antarctic Peninsula

Christian H. Fritsen · Jeramie C. Memmott ·

Robin M. Ross · Langdon B. Quetin ·

Maria Vernet · Eric D. Wirthlin

Received: 27 May 2010 / Revised: 1 November 2010 / Accepted: 2 November 2010 / Published online: 25 November 2010
© Springer-Verlag 2010

Abstract Understanding the flow of solar energy into ecosystems is fundamental to understanding ecosystem productivity and dynamics. To gain a better understanding of this fundamental process in the Antarctic winter sea ice, we produced a model that estimates the time-integrated exposure of seasonal Antarctic sea ice to PAR through the use of remotely sensed sea ice concentrations, sea ice movement and spatially distributed PAR calculations that account for cloud cover and have applied this model over the past three decades. The resulting spatially distributed estimates of sea ice exposure to PAR by mid-winter are evaluated in context of changes in the timing of sea ice formation that have been documented along the Western Antarctic Peninsula (WAP) region and its potential effects on the variation (seasonal and inter-annual) in the accumulation of sea ice algae in this region. The analysis shows the ice pack is likely to have large inter-annual variations (10–100 fold) in productivity throughout the autumn to winter transition in the sea ice along the WAP. Moreover, the pack ice is likely to have spatial structure in regards to biological processes that cannot be determined from analysis of sea ice concentration information alone. The resulting inter-annual variations in winter processes are

likely to affect the dynamics of Antarctic krill (*Euphausia superba*).

Keywords Sea ice · Antarctica · Ice Algae · Photosynthetically active radiation · Insolation

Abbreviations

PAR	Photosynthetically active radiation
TIEP	Time-integrated exposure to PAR
SIMCOs	Sea ice microbial communities
WAP	Western Antarctic Peninsula
Chl <i>a</i>	chlorophyll <i>a</i>
SO-GLOBEC	Southern Ocean Global Ocean Ecosystems Dynamics

Introduction

Sea ice algae partially support the base of the Antarctic food web and have the greatest potential to be the major new source of energy to the Antarctic food web during the winter—at a time when ecosystem energy resources are at their minimum. As such, it has been shown that feeding of overwintering larval Antarctic krill (*Euphausia superba*) on this resource occurs throughout the Southern Ocean (Daly 1990; Ross and Quetin 1991; Atkinson et al. 2002; Quetin and Ross 2003; Quetin et al. 2007). Energy input to the ice algal communities through exposure of the ice to photosynthetically active radiation (PAR) throughout the myriad of sea ice habitats (e.g. Horner 1984; Legendre et al. 1986; Thomas and Dieckmann 2002) and subsequent photosynthesis is likely to be a determinant (ultimate factor) of the abundance of algae that grows and

C. H. Fritsen (✉) · J. C. Memmott · E. D. Wirthlin
Desert Research Institute, 2215 Raggio Parkway,
Reno, NV 89512, USA
e-mail: Christian.Fritsen@dri.edu

R. M. Ross · L. B. Quetin
Marine Science Institute University of California at Santa Barbara, Santa Barbara, CA 93106, USA

M. Vernet
Scripps Institution of Oceanography, University of California San Diego, 9500 Gilman Drive, La Jolla, CA 92093, USA

accumulates in sea ice before winter onset (Hoshiai 1985; Fritsen et al. 1994; Dieckmann et al. 1998; Fritsen et al. 2008). Moreover, the exposure of the sea ice to PAR during the autumn to winter transition is determined mostly by the dynamic interacting variables of ice growth initiation and expansion, cloud cover dynamics and seasonal radiation decline that vary across latitudinal gradients throughout Antarctica.

To evaluate the variation in the exposure of sea ice to PAR during the autumn to winter period, we have produced a model that estimates the time-integrated exposure of seasonal Antarctic sea ice to PAR through the use of remotely sensed sea ice concentrations and spatially distributed PAR calculations that account for cloud cover over the past decades. The resulting spatially distributed estimates of sea ice exposure are evaluated in context of changes in the timing of sea ice formation that have been documented along the Western Antarctic Peninsula region (Stammerjohn et al. 2008) and its potential effects on the variation (seasonal and inter-annual) in the accumulation of sea ice algae (Fritsen et al. 2008) in this region.

The start of the winter season along the Western Antarctic Peninsula (WAP) can be functionally defined as the time when solar radiation is decreasing to its minimum and water column algae also reach their seasonal minimum (typically in May). Starvation tolerances and adaptations of the biota that rely on these water column algal resources are employed during the duration of the winter. Antarctic krill larvae along the WAP in the winter have starvation tolerances typically on the order of 4–5 weeks with the oldest larvae having a maximum of 10 weeks starvation survival period (Ross and Quetin 1991; Meyer and Oettl 2005; Quetin et al. 2007). Thus, our analysis of potential energy input into sea ice in austral winter is most relevant to the time period between the months of March (near the timing of the start of ice advance) and August/September. Similar analysis has also been applied to the Eastern Antarctic to estimate potential ice algal coupling to phytoplankton bloom development (e.g. Raymond et al. 2009) in the austral spring. We suggest that this approach can be used to better evaluate in situ data collections seeking to evaluate the dynamic coupling among phytoplankton, ice, ice algae and krill.

Materials and methods

Analytical approach

We have modeled the time-integrated exposure of sea ice to PAR over the time period of sea ice concentration data from satellites (1979–2006) using the daily insolation from PAR on to the surface of the sea ice and integrating

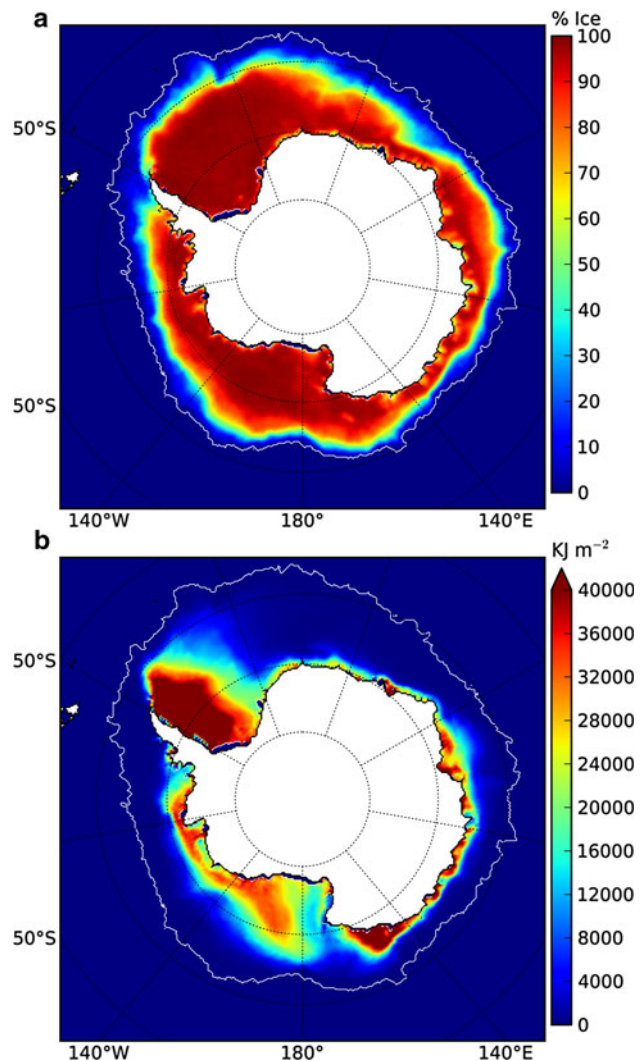


Fig. 1 **a** Mean sea ice concentration on June 21 and **b** the mean TIEP from March 1 to June 21 of each year over the years of 1979–2006. The maximum calculated mean TIEP from March 1 to June 21 in 1979–2006 was $\sim 90,000 \text{ kJ m}^{-2}$ in the areas of multi-year ice in the western Weddell Sea

this daily insolation, while taking into account variations in ice concentration and movement (Fig. 1b). Sea ice concentrations were derived using Bootstrap algorithm for sea ice concentrations from Nimbus-7 SMMR and DMSP SSM/I data (version 2) (Comiso 1999, updated 2008). The sea ice was classified into increments of 15% concentration (e.g. 15–30%, 30–45%) and ice concentrations less than 15% (Stammerjohn et al. 2008) were considered ice free. The ice exposure to PAR was calculated by multiplying the global PAR flux by the daylength for each ice class present within each pixel (presently using the $25 \times 25 \text{ km}$ resolution of the sea ice concentration data). The PAR flux was derived from the NASA/GEWEX Surface Radiation Budget (SRB) version 3.0 as obtained

from the NASA Langley Research Center Atmospheric Sciences Data Center NASA/GEWEX SRB Project. The SRB PAR data were distributed on a $1^\circ \times 1^\circ$ grid for the entire globe, and the PAR for each pixel was estimated using a 5th degree multivariate spline interpolation of the SRB data. Multivariate spline interpolation was selected over traditional linear methods in an effort to increase the accuracy of estimates (Kidner et al. 1999). The resulting interpolated PAR values were then multiplied by the daylength at each pixel location. Daylength was calculated according to Forsythe et al. (1995) as a function of latitude. In years prior to 1984 (the first-year SRB PAR product was available), we have used the approximation of PAR as the SRB PAR from 1984 or 1985 (dependent upon leap year status). The daily PAR exposure for each age-class of ice was then integrated daily as the season progressed such that the sea ice exposure to PAR over the season was integrated over time to yield the Time-Integrated Exposure to PAR (TIEP) at any given location within the ice pack. When ice was no longer present during the analysis period, the TIEP was reset to zero. These calculations assume that the youngest ice classes are the first to go away as ice concentrations at any specific location decrease.

To account for sea ice movement, the Polar Pathfinder Daily 25 km Equal-Area Scalable Earth Grid (EASE-Grid) Sea Ice Motion Vectors (Fowler 2003, updated 2007) were used to estimate the daily locations of the sea ice. Ice movement was estimated by applying the velocity vectors through 24 h of motion. The sea ice motion vectors (distributed on EASE-Grid) and the PAR flux after movement at the ice concentration grid locations were determined through a 5th order multivariate spline interpolation. The sea ice concentration data on the subsequent day were then used to determine whether sea ice was still present. If ice was present, the daily PAR fluxes were added to TIEP from the previous day. Again, if ice was no longer present, the sea ice TIEP for this location was reset to zero. The TIEP for each ice class was thus calculated and recorded independently on a daily basis from the start until the end date of each chosen simulation or analytical period. The TIEP of each ice class present at a location was weighted equally when calculating the mean TIEP at that location. These TIEP means from all represented ice classes were the values used for producing the figures and tables in this publication.

The TIEP for second-year and multi-year floes as well as land-fast ice not removed by the land mask was calculated during each simulation. However, these values represent only that TIEP accumulated during the model run and grossly underestimates the actual TIEP for the ice that was present before the simulation start dates (which for these analyses was March 1st).

Ice algal biomass

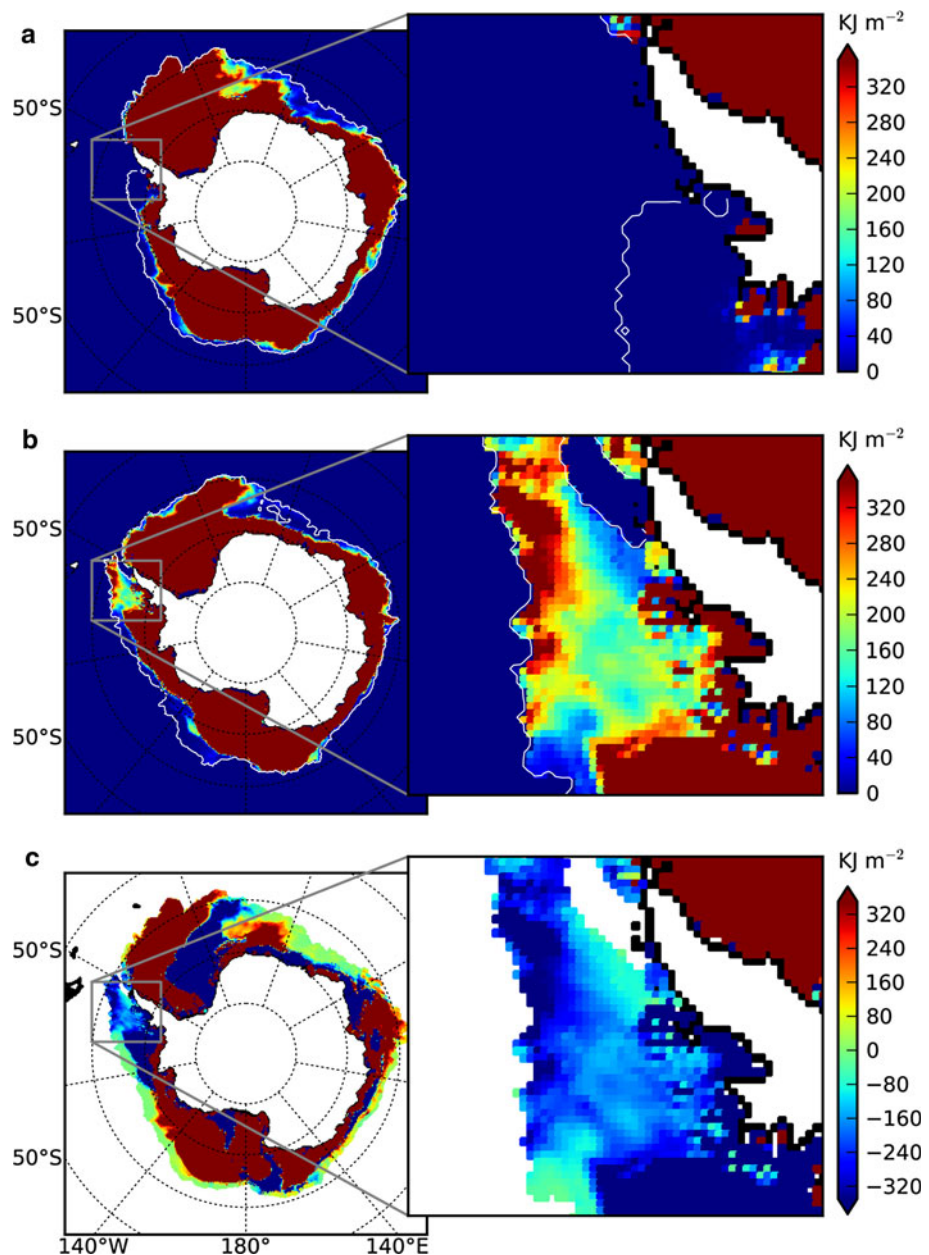
Sea ice cores collected for the determination of algal biomass were collected during the Southern Ocean GLOBEC (SO-GLOBEC, (Hofmann et al. 2002)) cruises in 2001 and 2002 (Fritsen et al. 2008). Chlorophyll *a* (Chl *a*) biomass from these cruises was compared to values of TIEP from the model results. A detailed description of the sampling methods, sample locations and biomass results was given by Fritsen et al. (2008). Briefly, sea ice cores were collected using seven-centimeter-diameter core barrels (Kovacs Enterprises). Some ice cores were sectioned before melting to evaluate the vertical distributions of biomass, while other cores were melted whole before analysis. Ice-core meltwater was filtered through GF/F filters, and filters were retained for analysis of Chl *a*. Filters were frozen (-80°C) until extraction in 90% acetone and analysis of Chl *a* content via fluorometry (Parson et al. 1984; Welschmeyer 1994).

Results

Dynamic interactions among ice dynamics and PAR

The dynamics of sea ice cover formation and expansion throughout the Southern Ocean is variable on an annual basis—but in general, the pack ice growth and expansion starts in February and March and the total extent typically exceeds 12–13 million km^2 by winter solstice (June 21). Expansion continues to a maximum of approximately 20 million km^2 by the end of August or early September (Fetterer et al. 2002, updated 2009). The dynamic interactions between the initial formation and the expansion of sea ice, cloud cover, ice movement and seasonal radiation decline are such that simple linear accumulations of TIEP do not occur over time nor space, either along the WAP or in other regions around the Southern Ocean (Fig. 1b). The Antarctic region with the highest TIEP for sea ice during the winter was consistently found in the western Weddell Sea (e.g. 67°S , 50°W)—where the maximum yearly mean for the evaluation period from March 1 to June 21 (season) was $\sim 90,000 \text{ kJ m}^{-2} \text{ season}^{-1}$ and typical values of greater than $50,000 \text{ kJ m}^{-2} \text{ season}^{-1}$ were observed. Other regions with typically high TIEP in mid-winter are located in the South Pacific Ocean east of the Balleny Islands (e.g. 68°S , 140°E) and in the Indian Ocean off the coast from the Amery Ice Shelf (e.g. 67°S , 75°E). These regions have estimated winter TIEP up to four orders of magnitude higher than that of the Western Antarctic Peninsula. The extremely high TIEP values in these regions are predominantly due to the perennial ice cover that receives very high PAR exposures during the early austral autumn.

Fig. 2 TIEP at winter solstice (June 21) for **a** 2001 and **b** 2002. The color scale's dynamic range is set to depict that found in the Western Antarctic Peninsula area (projected inset). On June 21, 2001 the maximum was ~0 and ~15,300 kJ m^{-2} on June 21, 2002. **c** The difference in TIEP between the years



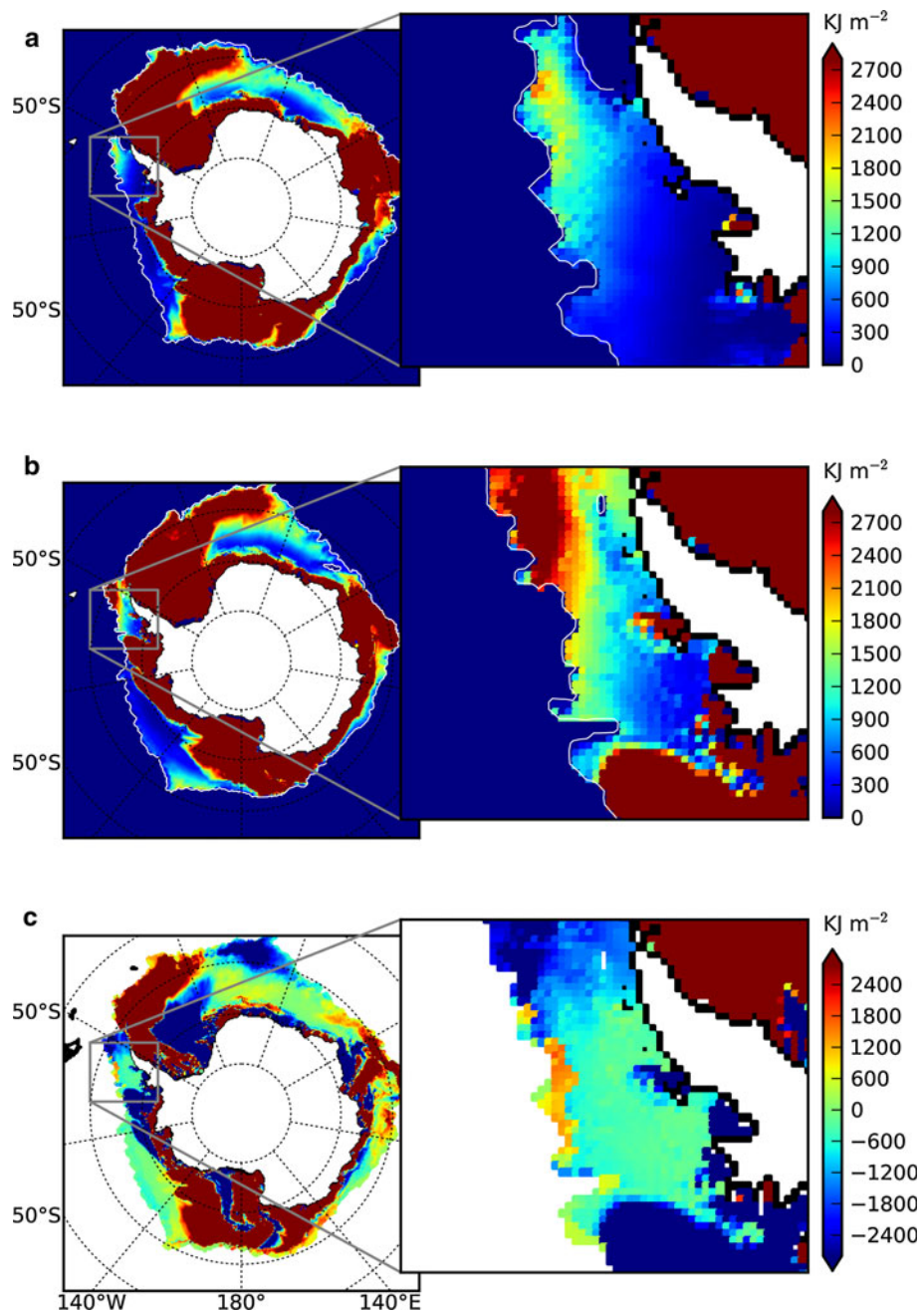
Regions with seasonal ice coverage (as opposed to perennial ice coverage) that typically exhibited high values for TIEP were found in the Indian Ocean, western Ross Sea and western Bellingshausen Sea and had values of $\sim 30,000 \text{ kJ m}^{-2}$ by winter solstice. These regions have relatively early ice formation when PAR is still available. Values for TIEP range from $\sim 10,000$ to $50,000 \text{ kJ m}^{-2}$ for these areas.

Regions typically exhibiting low TIEP during the fall-winter transition were found within the eastern Weddell Sea (e.g. 65°S , 10°W), the eastern Ross Sea (e.g. 70°S , 175°E) and the northern WAP (e.g. 65°S , 70°W) and had values of TIEP of less than $16,000 \text{ kJ m}^{-2}$ season $^{-1}$.

TIEP and sea ice-core chlorophyll *a*

Sea ice advance along the WAP occurred later in 2001 than 2002 (Stammerjohn et al. 2008) and a substantial portion of the sea ice in the region in 2001 formed after the mid-winter day lengths decreased to zero. Consequently, much of the ice along the WAP in 2001 was not exposed to any PAR during the fall-winter transition (Fig. 2). In contrast, ice formation in the WAP in 2002 had proceeded early enough such that the ice was exposed to PAR and the mean TIEP in the region was over four orders of magnitude higher (Figs. 2, 5) on June 21 than on the same date in 2001.

Fig. 3 Model estimate of TIEP on August first—a time at the beginning of the SO-GLOBEC winter cruises during 2001 (a) and 2002 (b) and the difference image (c). Maximum values were $\sim 1300 \text{ kJ m}^{-2}$ in 2001 and $\sim 9600 \text{ kJ m}^{-2}$ in 2002



Biomass data in the pack during winter are generally lacking—yet the SO-GLOBEC data were collected in late-winter early spring in 2001 and 2002. By the time that this sampling occurred, the sea ice in the region was beginning to experience moderate changes in the TIEP due to seasonally increasing solar radiation (Fig. 3). Increases mainly occurred along the northern extent of the pack ice in both years. Chl *a* within ice cores collected during these years in the Marguerite Bay region exhibited variations of 100-fold (Fig. 4). These variations are somewhat expected given the large variability in the spatial geophysical properties of the pack ice (Eicken et al. 1991). However, the statistical

distributions between the years exhibited a ten fold significant difference (Fritsen et al. 2008)—with the significantly higher biomass (Chl *a*) being in the ice cores collected in 2002—which coincided with roughly a ten fold difference in the mid-winter TIEP distributions calculated within the SO-GLOBEC study grid area (Fig. 4).

Inter-annual variability and trends along the WAP

The TIEP of sea ice along the WAP was at its highest levels in 1979–1981 with winter solstice sea ice accumulations of TIEP being greater than $2,000 \text{ kJ m}^{-2}$ well north

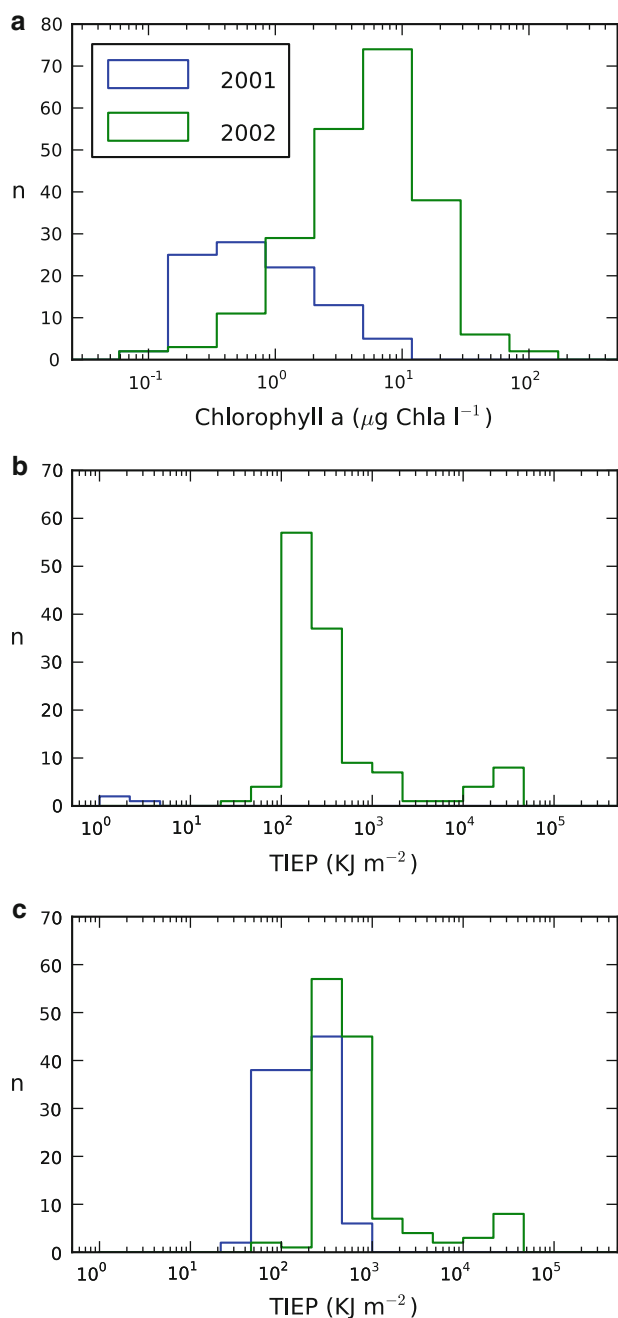


Fig. 4 Histograms showing relationship of ice-core Chl *a* and estimated TIEP in the SO-GLOBEC sampling area (Hofmann et al. 2002). **a** Mean Chl *a* for each core collected on the SO-GLOBEC 2001 and 2002 cruises **b** distribution of TIEP in the NBP sampling grid area on June 21st and **c** the distribution of TIEP in the NBP sampling grid on August 1st—at the beginning of the cruises

of Adelaide Island (Figs. 5, 6). A steady decrease was evident in the region until 1985 where the sea ice deep inside Marguerite Bay was the only in the WAP to experience large TIEP (Fig. 5; see inset panel for 1985). The annual average mid-winter TIEP for the region (Fig. 5) then increased with medium TIEP in 1986 and relatively

high values for TIEP in 1990. Conditions in 1991 were characterized by an abrupt increase in both TIEP and extent but, due to dynamic interactions with the timing of ice formation and PAR, the on-shelf region of the WAP had relatively little accumulation of TIEP. The TIEP in the WAP peaked again in 1992 and continued with annual average winter TIEP values that decreased gradually through 2001. The season with the sea ice having the second lowest TIEP occurred during 2001, where the ice extent was low and the timing of advance was substantially delayed relative to the average for the region. An abrupt increase in extent occurred in 2002 (also described by Stammerjohn et al. (2008)) and resulted in the largest year-to-year increase in the winter sea ice TIEP. The TIEP decreased in 2003 and 2004 to below average and then peaked in 2005 with TIEP similar to that of 2002. The last year with processed ice motion vector data available at the time this work was performed was for 2006, and the mid-winter sea ice TIEP was below average at $\sim 2 \text{ kJ m}^{-2}$. The long-term average TIEP in the WAP from 1979 to 2006 for the WAP was $\sim 360 \text{ kJ m}^{-2}$.

Discussion

Spatial and temporal structure may exist within the sea ice ecosystem and may be present due to the differential effects of the age of ice, ice movement and exposure to PAR. This apparent structure cannot be inferred by analysis of the sea ice concentration dynamics alone. Although ice concentration is a key element of the ecosystem structure—images of concentration alone have limited utility when interpreting potential differences in the energy distribution throughout the ice pack (Fig. 1). The timing of formation and the subsequent motion of the sea ice had the greatest impact on the distribution of TIEP during the fall-winter transition and early spring, where TIEP was mainly concentrated near shore unless movement and/or second-year ice was a factor (e.g. Weddell Sea).

Along the WAP, there has been an apparent decrease in the sea ice with TIEP at mid-winter throughout the satellite era (Fig. 5). A large decline was apparent in the mean TIEP from greater than $1,000 \text{ kJ m}^{-2}$ along the WAP in the early 1980s to much lower values in the last 20 years. Maxima occurred in 1987, 1992, 2002 and 2005 with high values greater than 300 kJ m^{-2} . This analysis of the TIEP may also indicate a cyclical nature to the TIEP in the WAP, running over an approximately 12-year interval with only two cycle minima being reached during the satellite era. The cyclical nature of the winter TIEP is mostly driven by the early ice formation dynamics and these are thought to be tied/linked to the Antarctic Circumpolar wave that is in turn tied to the global ocean and atmospheric

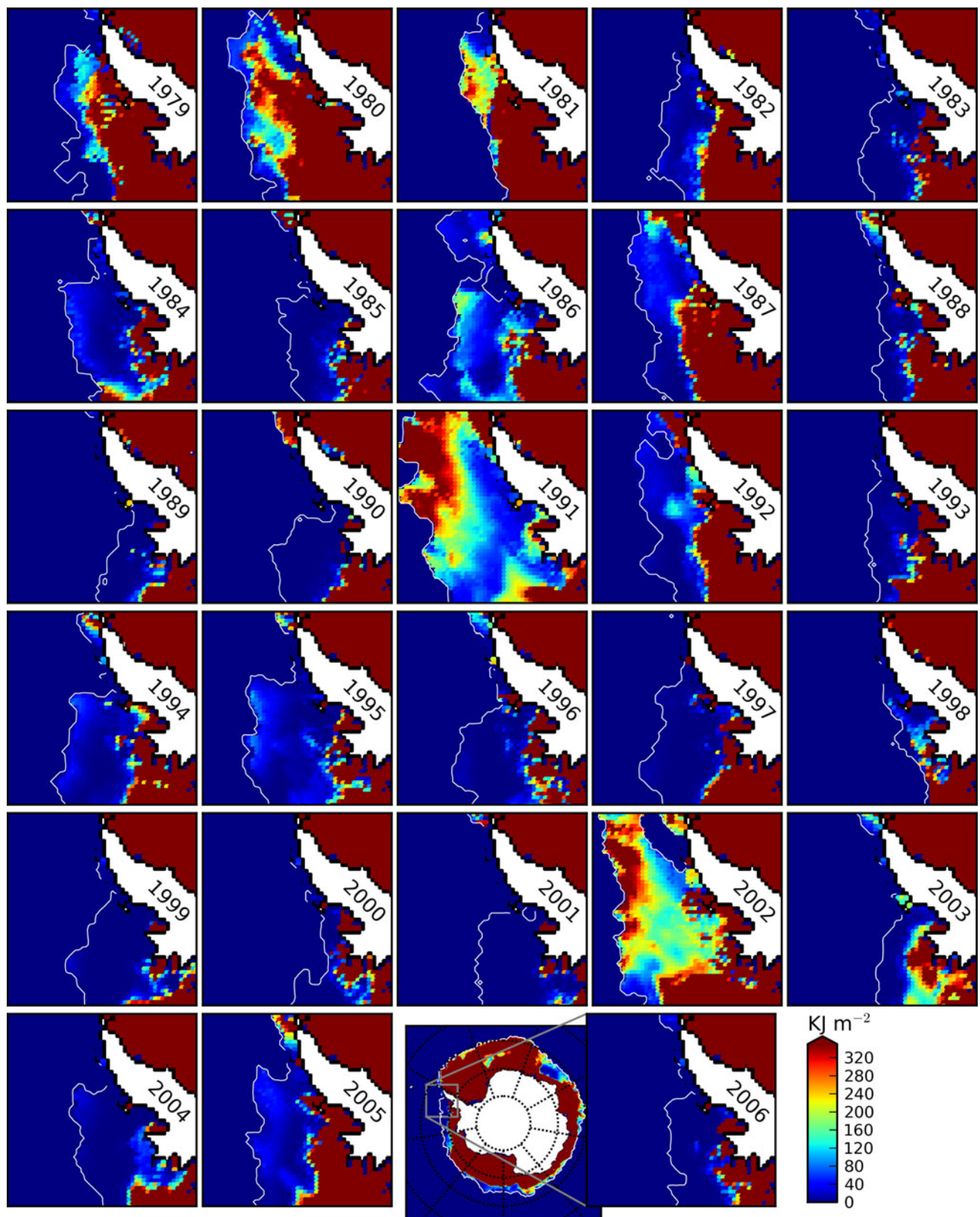


Fig. 5 Estimated TIEP from March 1 to June 21 for each year from 1979 to 2006 along the WAP

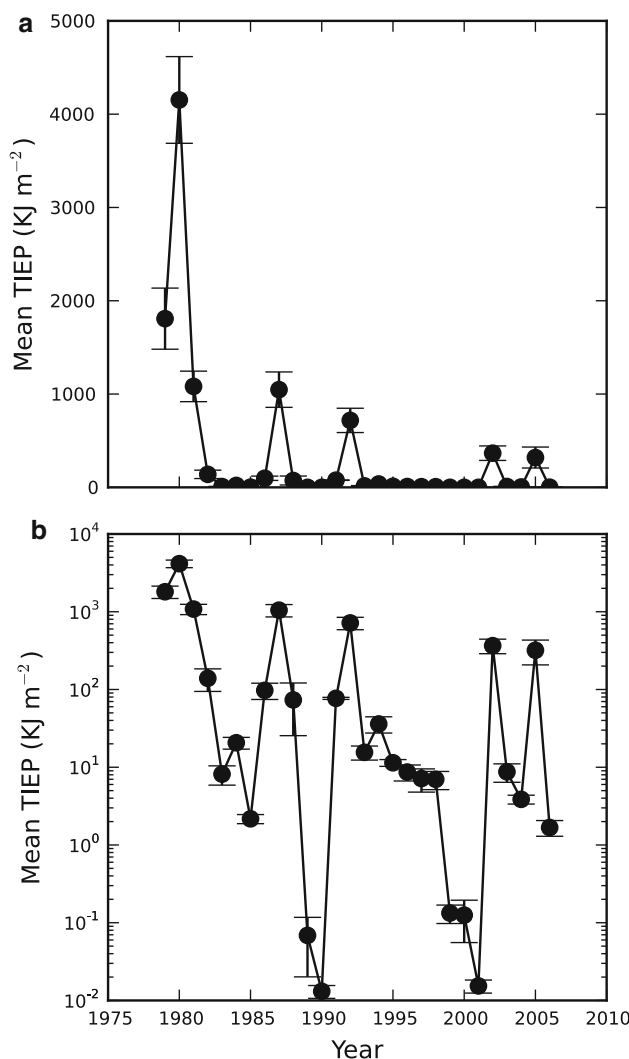


Fig. 6 Estimated mean of yearly TIEP from 03/01 to 06/21 for the area inside the Palmer LTER study area (Smith et al. 1995) expressed as the mean \pm standard deviation (a) and the same as shown in panel a but depicted with a log-scale projection to show the order of magnitude variation between years (b)

teleconnections that operate over similar time-scales (Stammerjohn et al. 2008).

TIEP and sea ice algal biomass

Processes affecting the accumulation of algal biomass in sea ice in the autumn include scavenging of algal biomass from seawater as ice is formed (Garrison et al. 1989; Ackley and Sullivan 1994), filtering of biomass from sea water through the pancake ice matrix as seawater interacts in the wave fields (Thomas and Dieckmann 2002), primary production and growth within sea ice in the autumn (Fritsen et al. 1994; Hoshiai et al. 1996) and losses due to both physical and biological processes (mortality, grazing, etc.). Biomass accumulation resulting from scavenging and

filtering is likely enhanced when ice is formed early in the season, due in part to higher biomass concentrations in seawater while light for photosynthesis in the water column is still available. The contribution of scavenging and filtration of algal biomass in sea ice and subsequent growth has not yet been accounted for in modeling efforts. Yet, differences in the initial standing stocks of algal biomass are likely to have substantial impacts on subsequent growth dynamics.

The biomass accumulated in early-forming sea ice may also increase through in situ production and algal growth as long as PAR is available for photosynthesis before complete winter darkness. The differences in TIEP in the WAP coinciding with the differences in the algal biomass in ice cores collected on the SO-GLOBEC cruises (Fig. 6a, c) suggest that the PAR is likely to be an ultimate factor influencing in situ growth and accumulation of sea ice algae on a regional scale. The difference in the mean TIEP in the SO-GLOBEC sampling region in 2001 and 2002 was roughly $2,600 \text{ kJ m}^{-2}$. Assuming an average albedo for the pack ice cover of 80% and converting the PAR energy from joules to quanta (2.77×10^{18} quanta per joule (Morel and Smith 1974)), we can compare the energy/photons available to the sea ice ecosystem with estimated differences in the algal carbon. Assuming a C: Chl *a* ratio of 75 (wt/wt), the differences between the average algal biomass in the ice were roughly $0.04 \text{ mol of C m}^{-2}$. An upper boundary for primary production and carbon fixation can be derived from the TIEP calculations (by making the most conservative assumptions; (1) that all of the PAR photons not reflected from the ice surface were to be absorbed and used in photosynthesis and (2) a maximum quantum yield of 0.1 mol C:mol quanta). Using this approach, a maximum theoretical difference in the carbon content of the sea ice algae between the years would be approximately $0.25 \text{ mol C m}^{-2}$. This number is perhaps not that useful, except in the sense that the PAR calculations can set an upper boundary to the expectations for primary production that might occur within the sea ice ecosystem. Perhaps more useful is the direct comparison of the changes in the TIEP and the sea ice algal carbon between the 2 years that allows the calculation of a quasi-apparent ecosystem quantum yield of $0.015 \text{ mol of carbon relative to the moles of photons entering the sea ice system}$. The extent to which there is a correspondence between the total integrated exposure of ice to PAR and ice algal biomass remains to be documented and determined. However, we might expect that this correspondence may not be linear as the sea-ice microalgal consortia become limited by other environmental limitations such as nutrients and CO₂ or space. Previous analysis however suggests that the autumn is a period when light limitations may be the primary determinant of algal growth (Arrigo et al. 1997).

The sea ice TIEP in regions with a high proportion of multi-year floes in winter was much higher than that in areas with seasonal ice (i.e. areas with newly forming first-year ice; Fig. 1). Subsequently, it is these regions, with multi-year floes, that may have the highest potential for primary productivity in the autumn and early winter. This result contrasts those for modeling potential sea ice algal blooms in the austral spring where the regions with the high proportion of multi-year floes having thick snow cover have the lowest estimated primary production (Arrigo et al. 1997). It is important to note that in early spring, the pack ice has experienced a winter season with many days of being exposed to freezing air temperatures, whereas the ice pack remaining through the summer and into the autumn has experienced many days of temperatures at or near freezing. The differences in the status of the ice pack during the two seasons are important to note because field studies in the pack ice in the autumn have shown that thick snow covers do not result in lower biomass or primary production. Rather, the snow cover creates flooding in isothermal ice and creates habitats near the surface of the ice that are often very productive (Meguro 1962; Fritsen et al. 1994; Thomas et al. 1998). Thus, this analysis suggests these regions with multi-year ice and ice with insulating snow covers may actually be some of most productive areas in the austral autumn and of great importance for overwintering biota. Results in Arrigo et al. (1997) also appear to support this assertion when examining their results for the months of March and April that show moderate productivities in regions known for perennial ice coverage.

Potential cascading effects

Variation in TIEP potentially has effects not only on the biomass of the algal component of the sea ice microbial communities (SIMCOs) but also on organisms dependent on SIMCOs as a food source. The concept that the life cycle of Antarctic krill (*Euphausia superba*) is tightly linked to the seasonal dynamics in sea ice has been in existence for decades (Smetacek et al. 1990) and algal biomass in sea ice has been postulated as an important food resource for larval krill (Daly 1990; Ross and Quetin 1991; Siegel and Loeb 1995) in winter when food availability in the water column is not likely adequate for survival. Based on observations from two contrasting winters during SO-GLOBEC, a strong linkage was shown among the accumulated Chl *a* biomass in the sea ice (cores), plant pigment in the guts of larval krill and the growth rates of larval krill (Quetin et al. 2007). Thus, it is not surprising that recruitment success of Antarctic krill is correlated with the timing of sea ice formation, duration of ice cover and sea ice extent (Siegel and Loeb 1995; Quetin and Ross

2003). TIEP from the model integrates several aspects of seasonal sea ice dynamics, including the timing of advance, the duration and the movement of the ice cover. Successful recruitment in Antarctic krill is highly variable and, when long-term data sets are available, has been shown to be episodic (Quetin and Ross 2003; Siegel et al. 2003). Modeling, estimating and tracking TIEP could be a valuable tool for forecasting krill recruitment success and population dynamics, particularly as seasonal sea ice dynamics change as a result of changing climate. The structure that these results reveal in the ice pack (e.g. Figs. 1, 2, 3, 5) indicates that TIEP might be used as a means to identify regions within the pack that are optimal for recruitment. The apparent downward trend shown in TIEP model results since 1979 is also observed in krill standing stocks in the south west Atlantic sectors of the Southern Ocean (Atkinson et al. 2004), but on the regional scale of the Palmer LTER study region (Smith et al. 1995), higher than average TIEP does not predict all of the observed successful year classes. The inclusion of scavenging data, filtering inputs and production estimates based on TIEP and ice class would add more realism to the model output and might further refine the evaluation of locations with optimal krill recruitment.

Future directions

The remotely sensed parameters used in the model (e.g. ice concentration) are currently available in much finer resolution than used in the model. Future refinement of the approach could include the use of the higher resolution data that exist for each year and update to newer, more refined products where available for comparison with the currently used methods. Snow cover algorithms if they were to be validated and be accurate for the Antarctic may also be incorporated. However, challenges remain in providing accurate remotely sensed snow-depth products (due in part to the flooding and freezing phenomena that occurs prolifically through the Southern Ocean).

Acknowledgments This research was supported by NSF-Office of Polar Programs grants ANT-0529666, ANT-0529087, and ANT-0528728. We thank the many contributors to engaging discussions regarding seasonal timing and potential ecosystem response over the past seasons.

References

- Ackley SF, Sullivan CW (1994) Physical controls on the development and characteristics of Antarctic sea ice biological communities: a review and synthesis. Deep Sea Res part 2 Top Stud Oceanogr 41:1583–1604
- Arrigo KR, Worthen DL, Lizotte MP, Dixon P, Dieckmann G (1997) Primary production in Antarctic sea ice. Science 276:394–397

- Atkinson A, Stubing D, Hagen W, Schmidt K, Bathmann UV (2002) Feeding and energy budgets of Antarctic krill *Euphausia superba* at the onset of winter- II. Juveniles and adults. Limnol Oceanogr 47:953–966
- Atkinson A, Siegel V, Pakhomov E, Rothery P (2004) Long-term decline in krill stock and increase in salps within the Southern Ocean. Nature 432:100–103
- Comiso J (1999, updated 2008) Bootstrap sea ice concentrations from NIMBUS-7 SMMR and SMSR SSM/I, 01 March 1979 to 31 December 2007. National Snow and Ice Data Center, Boulder, CO USA, Digital Media
- Daly KL (1990) Overwintering development, growth, and feeding of larval *Euphausia superba* in the Antarctic marginal ice zone. Limnol Oceanogr 35:1564–1576
- Dieckmann GS, Eicken H, Haas C et al (1998) A compilation of data on sea ice algal standing crop from the Bellingshausen, Amundsen and Weddell Seas from 1983 to 1994. In: Lizotte MP, Arrigo K (eds) Antarctic Sea ice biological processes, interactions, and variability, vol 73. Am Geophys Union, Washington, pp 85–92
- Eicken H, Lange MA, Dieckmann GS (1991) Spatial variability of sea-ice properties in the northwestern Weddell Sea. J Geophys Res 96:10603–10615
- Fetterer F, Knowles K, Meier W, Savoie M (2002, updated 2009) Sea ice index. National Snow and Ice Data Center, Boulder, CO USA, Digital Media
- Forsythe WC, Rykiel EJJ, Stahl RS, Wu H-i, Schoolfield RM (1995) A model comparison for daylength as a function of latitude and day of year. Ecol Model 80:87–95
- Fowler C (2003, updated 2007) Polar pathfinder daily 25 km EASE-grid sea ice motion vectors national snow and ice data center, Boulder, CO USA, Digital media
- Fritsen CH, Lytle VI, Ackley SF, Sullivan CW (1994) Autumn bloom of Antarctic pack-ice algae. Science 266:782–784
- Fritsen CH, Memmott J, Stewart FJ (2008) Inter-annual sea-ice dynamics and micro-algal biomass in winter pack ice of Marguerite Bay, Antarctica. Deep Sea Res part 2 Top Stud Oceanogr 55:2059–2067
- Garrison DL, Close AR, Reimnitz E (1989) Algae concentrated by frazil ice: evidence from laboratory experiments and field measurements. Antarct Sci 1:313–316
- Hofmann EE, Klinck JM, Costa DP et al (2002) U.S. Southern ocean global ocean ecosystems dynamics program. Oceanography 15:64–74
- Horner R (1984) Phytoplankton abundance, chlorophyll a, and primary productivity in the western Beaufort Sea. In: Barnes PW, Schell DM, Reimnitz E (eds) The Alaskan Beaufort Sea: ecosystems and environments. Academic Press, London, pp 295–310
- Hoshiai T (1985) Autumnal proliferation of ice-algae in Antarctic sea-ice. In: Siegfried WR, Condy PR, Laws RM (eds) Antarctic nutrient cycles and food webs. Springer, Berlin, pp 89–92
- Hoshiai T, Tanimura A, Kudoh S (1996) The significance of autumnal sea ice biota in the ecosystem of ice-covered polar seas. Polar Biol 9:27–34
- Kidner D, Dorey M, Smith D (1999) What's the point? Interpolation and extrapolation with a regular grid DEM. http://www.geocomputation.org/1999/082/gc_082.htm
- Legendre L, Rochet M, Demers S (1986) Sea-Ice microalgae to test the hypothesis of photosynthetic adaptations to high frequency light fluctuations. J Exp Mar Biol Ecol 97:321–326
- Meguro H (1962) Plankton ice in the Antarctic Ocean. Rep Japanese Antarct Res Expedition. 1192–1199
- Meyer B, Oettl B (2005) Effects of short-term starvation on composition and metabolism of larval Antarctic krill *Euphausia superba*. Mar Ecol Prog Ser 292:263–270
- Morel A, Smith RC (1974) Relation between total quanta and total energy for aquatic photosynthesis. Limnol Oceanogr 19:591–600
- Parson TR, Maita Y, Lalli CM (1984) A manual of chemical and biological methods for seawater analysis. Pergamon Press, Oxford
- Quetin LB, Ross RM (2003) Episodic recruitment in Antarctic krill, *Euphausia superba*, in Palmer LTER study region. Mar Ecol Prog Ser 259:185–200
- Quetin LB, Ross RM, Fritsen CH, Vernet M (2007) Ecological responses of Antarctic krill to environmental variability: can we predict the future? Antarct Sci 19:253–266
- Raymond B, Meiners K, Fowler CW et al (2009) Cumulative solar irradiance and potential large-scale sea ice algae distribution off East Antarctica (30°A degrees E–150°A degrees E). Polar Biol 32:443–452. doi:[10.1007/s00300-008-0538-5](https://doi.org/10.1007/s00300-008-0538-5)
- Ross RM, Quetin LB (1991) Ecological physiology of larval Euphausiids, *Euphausia superba* (Euphausiacea). Mem Queensl Mus 31:321–333
- Siegel V, Loeb V (1995) Recruitment of Antarctic krill *Euphausia superba* and possible causes for its variability. Mar Ecol Prog Ser 123:45–56
- Siegel V, Ross RM, Quetin LB (2003) Krill (*Euphausia superba*) recruitment indices from the western Antarctic Peninsula: are they representative of larger regions? Polar Biol 26:672–679. doi:[10.1007/s00300-003-0537-5](https://doi.org/10.1007/s00300-003-0537-5)
- Smetacek V, Scharek R, Nothig EM (1990) Seasonal and regional variation in the pelagic and its relationship to the life history cycle of krill. In: Kerry KR, Hempel G (eds) Antarctic ecosystems: ecological change and conservation. Springer, Berlin, pp 103–114
- Smith RC, Baker KS, Fraser WR et al (1995) The Palmer LTER: a long-term ecological research program at Palmer Station, Antarctica. Oceanography 8:77–86
- Stammerjohn SE, Martinson DG, Smith RC, Iannuzzi RA (2008) Sea ice in the Western Antarctic Peninsula region: spatio-temporal variability from ecological and climate change perspectives. Deep Sea Res Part 2 55:2041–2058. doi:[10.1016/j.dsro.2008.04.026](https://doi.org/10.1016/j.dsro.2008.04.026)
- Thomas DN, Dieckmann GS (2002) Antarctic sea ice—a habitat for extremophiles. Science 295:641–644
- Thomas DN, Lara RJ, Haas C et al (eds) (1998) Biological soup within decaying summer sea ice in the Amundsen Sea, Antarctica. American Geophysical Union, Washington
- Welschmeyer NA (1994) Fluorometric analysis of chlorophyll a in the presence of chlorophyll b and pheopigments. Limnol Oceanogr 39:1985–1992